EVIDENCE FOR EXPOSED WATER FROST IN THE MOON'S SOUTH POLAR REGIONS FROM LRO ULTRAVIOLET ALBEDO AND TEMPERATURE MEASUREMENTS. P. O. Hayne[1] and A. Hendrix[2], E. Sefton-Nash[3], P. G. Lucey[4], K. D. Retherford[5], J-P. Williams[3], M. A. Siegler[1], B. T. Greenhagen[1], D. A. Paige[3], [1]Jet Propulsion Laboratory, California Institute of Technology (Paul.O.Hayne@jpl.nasa.gov), [2]Planetary Science Institute, [3]University of California, Los Angeles, CA, [4]University of Hawii, [5]Southwest Research Institute

Introduction: We investigated the relationship between lunar surface and subsurface temperatures and UV albedo spectra, using data from LRO's Diviner [*1*] and Lyman-Alpha Mapping Project (LAMP) [*2*]. Temperature data from Diviner, along with thermal models, constrain the locations where water ice would be thermodynamically stable, and the LAMP albedo data constrain the presence and abundance of water frost at the optical surface [*3*]. Diviner data present an opportunity to test the hypothesis that temperature controls the distribution of water frost in the Moon's polar regions. If water frost is present at the surface, this could represent a valuable resource for future *in situ* extraction and scientific analysis or resource utilization. Therefore, improved knowledge of the distribution of surface frost on the Moon would enable future missions to study and utilize lunar volatiles.

Data: Both the Diviner and LAMP datasets used here have high quality measurements for the lunar south polar region. LAMP uses stellar illumination sources to measure the UV reflectance of the lunar night side and polar regions. Due to the prevalence of UV-bright stars in the Moon's southern hemisphere, LAMP acquires data with much better signal-to-noise ratio (SNR) near the south pole.

Diviner. Diviner is a nine-channel filter radiometer, with spectral channels spanning wavelengths from ~0.3 to >100 μm [*4*]. We calculate and map bolometric brightness temperature, the wavelength-integrated radiance in all seven thermal Diviner channels expressed as the temperature of an equivalent blackbody [*1*]. To produce gridded map products from many observations, each observation is modeled as a Monte Carlo distribution of 100 points, each representing 1/100th of the original observation [*5*]. Bolometric brightness temperature are gridded to produce annual maximum and average bolometric brightness temperature maps (Fig. 1).

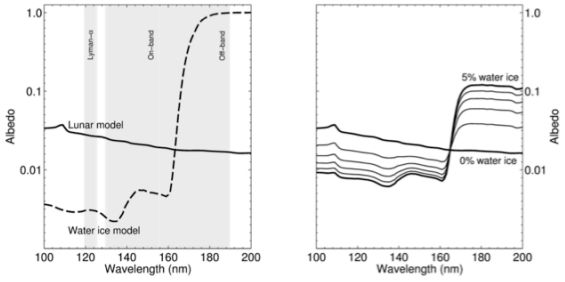

Figure 2: The effect of water ice concentration on measured LAMP spectra, based on the model described in the text. Ice and regolith are modeled as an intimate mixture.

LAMP. LAMP measures ultraviolet radiation reflected from the lunar surface, where the illumination source is a combination of starlight and emission from interplanetary hydrogen. We used publicly available gridded polar LAMP data products from NASA's Planetary Data System (PDS), dated 6 March, 2011. These gridded data records (GDR) consist of average albedo and statistical uncertainties in 250 meter-per-pixel bins, within four spectral bands: Lyman-α (119.57–125.57 nm), full stellar (129.57–189.57 nm), "on-band" (129.57–155.57 nm), and "off band" (155.57–189.57 nm). The off-band and on-band wavelengths refer to the position of a strong water absorp-

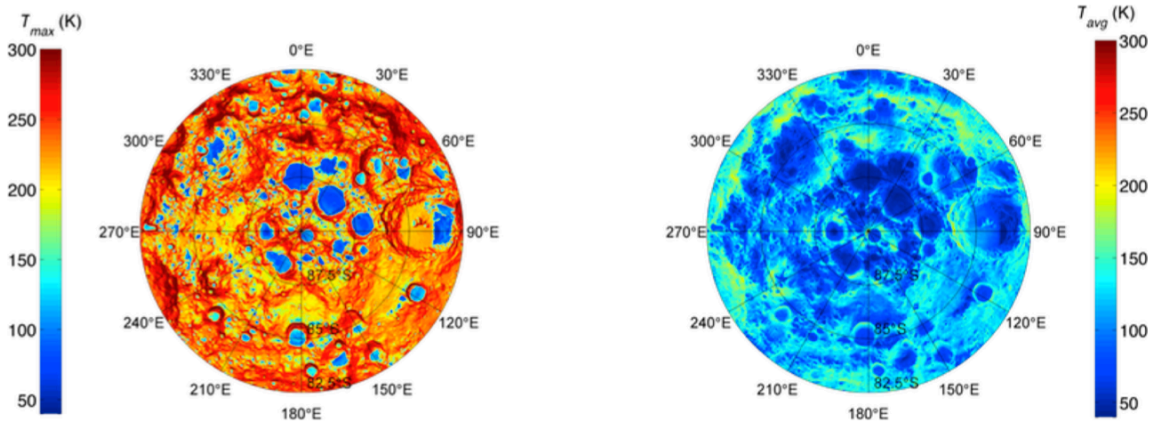

Fig. 1: Annual maximum (left) and average (right) surface temperatures from Diviner south polar measurements

tion feature, such that water frost has near-zero albedo in the on-band region, and albedo near-unity in the off-band region [*6*]. Therefore, the off-band/on-band ratio is expected to be high where any water frost is present on the surface [*3*]. To derive H_2O abundances from the measurements, we employed the albedo model of [*7*], with optical constants for water ice from [*8*] and dry regolith from [*6*]. Fig. 2 shows the effect of increasing water ice content on the expected UV reflectance spectrum.

Results: For locations with annual maximum temperatures T_{max} greater than the H_2O sublimation temperature of ~110 K, we find no evidence for exposed water frost, based on the LAMP UV spectra. For T_{max} < ~110 K, we find a strong correlation between decreasing T_{max} and apparent surface H_2O abundance (Fig. 3). Evidence for water frost comes from the following spectral features: a) decreasing Lyman-a albedo, b) decreasing "on-band" (129.57 – 155.57 nm) albedo, c) increasing "off-band" (155.57 – 189.57 nm) albedo, and d) increasing off-band/on-band ratio. All of these features are consistent with the UV spectrum of water ice, and are expected for water ice layers > ~100 nm in thickness. High regolith porosity, which would darken the surface at all wavelengths, cannot explain the observed spectral variations with temperature.

Given the observed LAMP off-band/on-band albedo ratios at a spatial scale of 250 m, the range of water ice concentrations within the cold traps with T_{max} < 110 K is ~0.1–2.0% by mass, if the ice is intimately mixed with dry regolith. If pure water ice is exposed instead, then up to ~10% of the surface area on the 250-m scale of the measurements may be ice-covered. The observed distribution of exposed water ice is highly heterogeneous, with some cold traps < 110 K having little to no apparent water frost, and others with a significant amount of water frost (Fig. 4). As noted by [*3*], this heterogeneity may be a consequence of the fact that the supply rate of H_2O molecules to the lunar poles is very similar to the destruction rate within the cold traps. However, an observed increase in apparent H_2O abundance with decreasing temperature from ~110 K to 65 K suggests that sublimation is the dominant loss process, and the rate of desorption of OH by UV photolysis may have been overestimated. We find a bimodal distribution of apparent ice concentrations with temperature, possibly due to the increasing importance of impact gardening for T_{max} < ~90 K. Finally, we cannot rule out the possibility that the colder population of ice deposits is in fact primarily carbon dioxide ice, although peak temperatures of ~65 K are slightly higher than the usual CO_2 sublimation temperature of ~60 K.

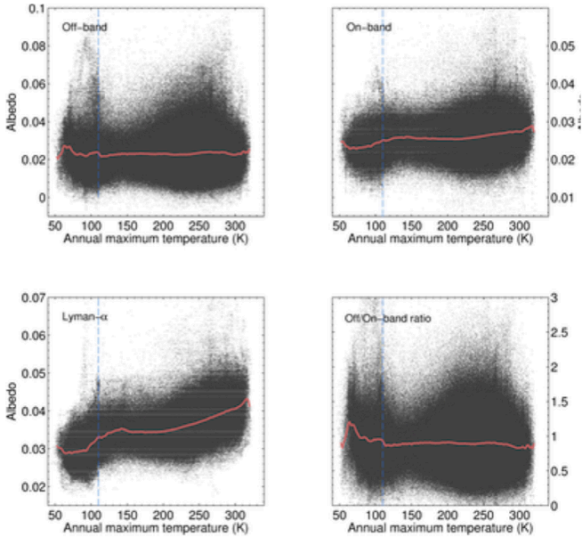

Figure 3: Ultraviolet spectral variations with temperature, for the three LAMP wavelength bands affected by the presence of

References: [1] Paige et al., *Space Sci. Rev., 150*, 2010. [2] Gladstone et al., *Space Sci. Rev.*, *150*, 2010. [3] Gladstone et al., *JGR*, *117*, 2012. [4] Paige et al., *Science*, *330*, 2010. [5] Sefton-Nash et al., *LPSC, 45*, 2014. [6] Hendrix et al., *JGR*, *117*, 2012. [7] Warren and Wiscombe, *J. Atmos. Sci.*, *37*, 1980. [8] Warren and Brandt, *JGR*, *113*, 2008.

Acknowledgment: *Part of this work was performed at the Jet Propulsion Laboratory, California Institute of Technology, under contract with the National Aeronautics and Space Administration*

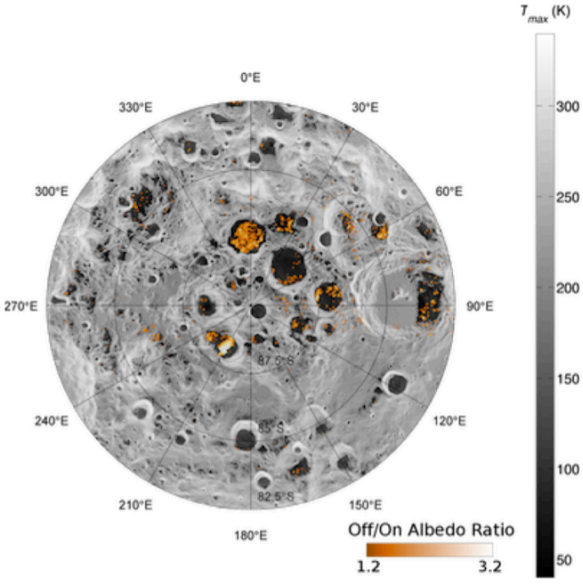

Figure 4: Distribution of exposed water frost, based on LAMP UV spectra having: a) Lyman-a albedo < 0.03, and b) off/on albedo ratio > 1.2. Note the strong correlation with the lowest temperature cold traps (grayscale indicates annual maximum temperature).